

Void fraction and flow regime determination by means of MCNP code and neural network

Ali Rabiei,
Mojtaba Shamsaei,
Mahdi Kafaee,
Mostafa Shafaei,
Naser Mahdavi

Abstract. One of the non-intrusive and accurate methods of measuring void fraction in two-phase gas liquid pipe flows is the use of the gamma-transmission void fraction measurement technique. The goal of this study is to describe low-energy gamma-ray densitometry using an ^{241}Am source for the determination of void fraction and flow regime in water/gas pipes. The MCNP code was utilized to simulate electron and photon transport through materials with various geometries. Then, a neural network was used to convert multi-beam gamma-ray spectra into a classification of the flow regime and void fraction. The simulations cover the full range of void fraction with Bubbly, Annular and Droplet flows. By using simulation data as input to the neural networks, the void fraction was determined with an error less than 3% regardless of the flow regime. It has thus been shown that multi-beam gamma-ray densitometers with a detector response examined by neural networks can analyze a two-phase flow with high accuracy.

Key words: flow regime • gamma-ray densitometry • neural network (NN) • Monte Carlo n-particle (MCNP) • void fraction

Introduction

The determination of the void fraction and flow regime in a two-phase mixture is of great importance in a variety of engineering application. It is essential to monitor flow regimes for the purpose of enhancing safety and overall performance in industrial systems such as nuclear reactors, petroleum and biomedical processing systems. Many researchers have been working on developing objective methodologies for flow regime identification. Hewitt [6] and Lahey and Banerjee [8] have reviewed various methods for measuring void fraction. Among them the radiation attenuation method as gamma-densitometry is a non-intrusive technique.

Measurement of the void fraction, i.e. the gas fraction, with traditional gamma-ray densitometers consist of a single source with one detector installed diametrically opposite it, are strongly dependent on the flow regime. Dependence on particular type of flow regime is significantly reduced by using multi-beam low-energy gamma-ray measurement principle [1].

Several beams from one low-energy source were used in our study; ^{241}Am with 59.5 keV gamma-ray emission. When gamma-ray photons pass through matter, they interact mainly through the photoelectric effect, Compton scattering and pair production [12]. The photoelectric effect and Compton scattering are the dominant interaction mechanisms for low-energy photons. Photoelectric interaction probability is proportional to the atomic number to the power of 4–5.

A. Rabiei, M. Shamsaei, M. Kafaee, N. Mahdavi
Physics Department,
Amirkabir University of Technology,
Tehran, Iran

M. Shafaei✉
Department of Nuclear Engineering,
Science and Research Branch,
Islamic Azad University,
Tehran, Iran,
Tel./Fax: +98 214 481 7170 4,
E-mail: mostafa.shafaei@gmail.com

Received: 23 October 2011

Accepted: 23 January 2012

The probability of a Compton interaction with an electron decreases with increasing photon energy and is independent of the atomic number of the interacting material and mainly depends on the electron density per unit mass [4].

Photon scattering is often regarded as an unwanted effect in gamma-ray transmission measurements, since it complicates the interpretation of the results. Build-up, i.e. the extra contribution to the measured transmission intensity from scattered radiation, has to be accounted for, particularly if wide-beam measurement configurations are used. In fluid flow fraction measurements, however, it is possible to take advantage of this effect since it effectively means that the gas-liquid distribution outside of the actual measurement volume affects the result [1].

For further analysis of the gamma-ray spectra, artificial neural networks were used, which are known to be applicable to the recognition and classification of a wide range of situations, patterns and individual features of different systems. Neural networks were trained on the simulated gamma-ray data and then used to analyze the measured spectra. This analysis enabled us to determine the void fraction with high accuracy for all the flow regimes and the flow regimes in the data set will be identified.

Simulation models

In two-component flows in which the components have sufficiently different densities, gamma densitometers can be used to measure the volume fractions, e.g. the gas fraction of the flow components. The void fraction is defined as the gas volume fraction divided by total volume of the flow as follows:

$$(1) \quad \alpha = \frac{V_g}{V} = \frac{V_g}{V_g + V_l}$$

$$V = V_g + V_l$$

where V is the total volume of the flow and V_g , V_l are the volume of gas and liquid, respectively.

Three basic flow regimes were simulated: Bubbly, Annular and Droplet flows. It was necessary to develop a model for each type of flow regime because of the difference in geometry. Each model includes a variable, which

allows the void fraction to be varied from 0 to 100%. In all flow regimes two cylinders defined the pipelines. The pipe wall material is aluminum and the inner and outer diameters of the pipe are 80 and 90 mm, respectively. In addition, cylinders were used to define the configuration of the detectors. Only idealized flow regimes have been considered in this paper in order to simplify the calculations. The Bubbly two-phase flow pattern appears to exist over a wide range of gas and liquid flow rates. Two-phase Bubbly flow is commonly defined as a flow pattern in which the dispersed gas bubbles spread in a continuum liquid with the bubble size smaller than the pipe diameter [2]. In ideal Bubbly flows spheres were used to define the bubbles so that the number of the bubbles could be altered. Generally, Annular flow can be viewed as separated flow when gas flow is not too fast. The major characteristic of Annular flow is the liquid film thickness that can be easily calculated from the void fraction [7]. For ideal Annular flows, a single cylinder was used to define the gas interface so that the dimension of the gas core could be changed. Spheres were used to define the liquid droplets in droplet flows so that the number of the liquid droplets could be chosen in order to define the void fraction. These flow regimes are shown in Fig. 1.

A 14 mCi ^{241}Am (59.5 keV) source and four CZT (CdZnTe) semiconductor detectors were used around the pipe at 180° , 140° , 68° and 52° with respect to the source position at 0° on the periphery of a given cross sectional area. The circular CZT detectors were of diameter 0.34 cm and the thickness of 2 mm.

Because of the large band gap of the CZT detectors, it can be operated at room temperature. As a result, the detector does not need to be cooled by liquid nitrogen during measurement. It means a spectroscopy system with a CZT detector is relatively compact. A CZT crystal in the detector has a density of 5.86 g/cm^3 and atomic percentage of 45.0% (Cd), 5.0% (Zn), and 50.0% (Te), respectively.

Artificial neural networks (ANNs)

ANNs are one of the most accurate and widely used nonlinear modeling tools. An ANN is a computational mechanism capable of representing continuous mapping

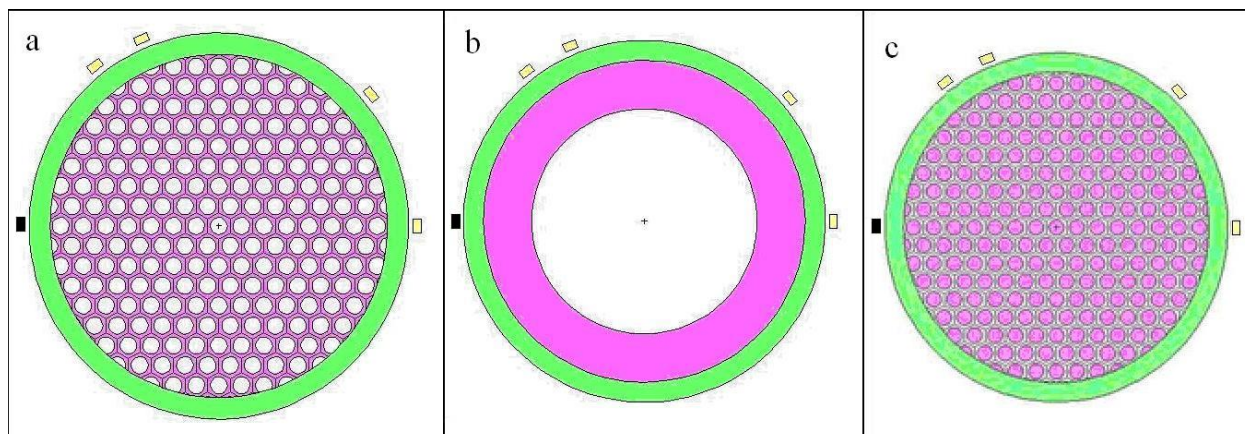


Fig. 1. Three different geometries due to Bubbly (a), Annular (b) and Droplet (c) flow regimes. The marginal grey rectangular boxes are detectors and the black rectangular box is a source.

from one multidimensional space of data to another by a set of given data representing that mapping. The ANNs are mathematical models that emulate some of the observed properties of biological nervous systems and draw on the analogies of adaptive biological learning [11]. The network is a structure of interconnected computational units which are called neurons, acting independently and simultaneously. The processing capability of the network is usually stored in inter-connection strengths called synaptic weights.

There are many ANN architecture each of them is suitable for a special type of problems. In most ANN modeling cases, such as this work, a very basic ANN model known as the multilayer perceptron (MLP) network is applied. MLPs consist of collection of simple processor units called neurons arranged in some layers. The neurons in one layer are fully connected to the neurons of next layer through weighted connections. In other words, outputs of neurons in one layer are inputs of neurons in the next layer. A neuron typically performs a nonlinear weighted sum of its inputs. Then, the result is passed through a transfer function to produce single output.

In a three-layer MLP, the neuron outputs of the first layer feed hidden layer neurons and the latest neurons feed neurons of the last layer. A one hidden layer ANN can model any nonlinear mapping with a finite number of discontinuities to any arbitrary level of accuracy if a sufficient number of neurons are assigned to its hidden layer. The number of hidden layers and the number of neurons in each hidden layer determine the capacity of the network, being usually determined through experimentation.

In the MLPs, at first, weights are randomly selected, and finally they can be determined adaptively by many supervised learning algorithms. One of the best of them is backpropagation algorithm. The learning algorithm adjusts weights and biases to handle a given example input/output data [5]. In fact, training minimizes the quadratic error between the network output and the desired output. With this approach, most of the computation effort is expended during the training process. Once trained, the operation of an MLP is accomplished through vector-matrix multiplication and application of nonlinear functions resulting in its fast operation. If a further speed increase is necessary, a trained MLP can be implemented in some of the most basic hardware digital signal processors (DSPs).

Generation of simulated data

MCNP is a general-purpose, continuous-energy, generalized-geometry, time-dependent, coupled n-particle, neutron, photon and electron, Monte Carlo (MC) transport code [3]. A system is defined by generating cells bounded by surfaces in three dimensions (3-D). Any kind of geometry can be defined as a cell and this cells can be rotated and moved to anywhere in the space.

The MC simulation models have been developed and implemented in order to study transmitted and scattered photons over the pipe cross-section [1]. Measuring the spectral detector response at several positions around the pipe allows the transmitted and scattered photons to be detected in several positions.

Pulse height analysis is used to study the energy depositions in the detectors. Once the detector responses have been combined and utilized, the void fraction and flow regime can be determined.

Figure 2 shows the spectra of different flow regimes at detector positions of 180°, 140°, 68° and 52° simulated with MCNP code when the void fraction alters from 0 to 100%. The collimated beam covered angles from 180° to 140°. Outside the beam the number of detected photons are smaller but not negligible. Only scatter photons are in these positions. Due to the different geometries of the flow regimes, the energy distribution of scattered photons reaching the detectors may differ between flow regimes. Thus, the spectra of detectors contain information about the flow regime.

ANN based modeling

In this non-invasive void fraction measuring system, there is one to one mapping between every void fraction in a special regime type and the obtained corresponding spectra. There are some clear peaks in the spectra: for detectors at 180° and 140°, the two peaks of 50 and 59.5 keV are selected as network inputs and for other detectors laying outside of beam collimation, the peak of 50 keV is chosen. These energies can be seen in Fig. 2. The counts of these energies and summation of counts of all energies (total count) of the spectra at the four detectors at every void fraction in every regime are selected as the input of the network.

Void fraction values and a number of regime types are considered as network outputs. Two separated ANNs with the same structure and same input are used, the first for void fraction prediction and the second for regime type classification. The output of the first network determines the void fraction and output of the second network determines the regime type. The structure of the MLP network consists of one 7 neurons input layer and one hidden layer with 20 neurons and one output layer with 1 neuron. All network inputs except the last one receive the counts of the peaks. The last input receives the summation of counts of 40 to 59.5 keV at the detectors; i.e. summation of the total count of the four detectors. Transfer functions of neurons are hyperbolic tangent sigmoid in the hidden layer and linear in the output layer.

Learning algorithm in this work is the Levenberg-Marquardt backpropagation [9, 10]. This fast iterative algorithm is based on gradient descent and it can reduce network error function by modifying the weights and biases in each iteration or epoch. Training and testing are done using the MATLAB Neural Network Toolbox.

Various void fraction MCNP simulations in different regimes, provide 117 data. But there are a few repetitive data. There is no difference between 3 simulated spectra corresponding to 0% void fraction in every regime and for the 100% is the same. In these cases various regime types are meaningless. Therefore, there are 4 repetitive data in these 6 mentioned cases which should be eliminated. They change the one to one mapping to another and in this condition a neural network cannot model it. After elimination of these repetitive data, 90 data were used as training data and 20 data were used as testing

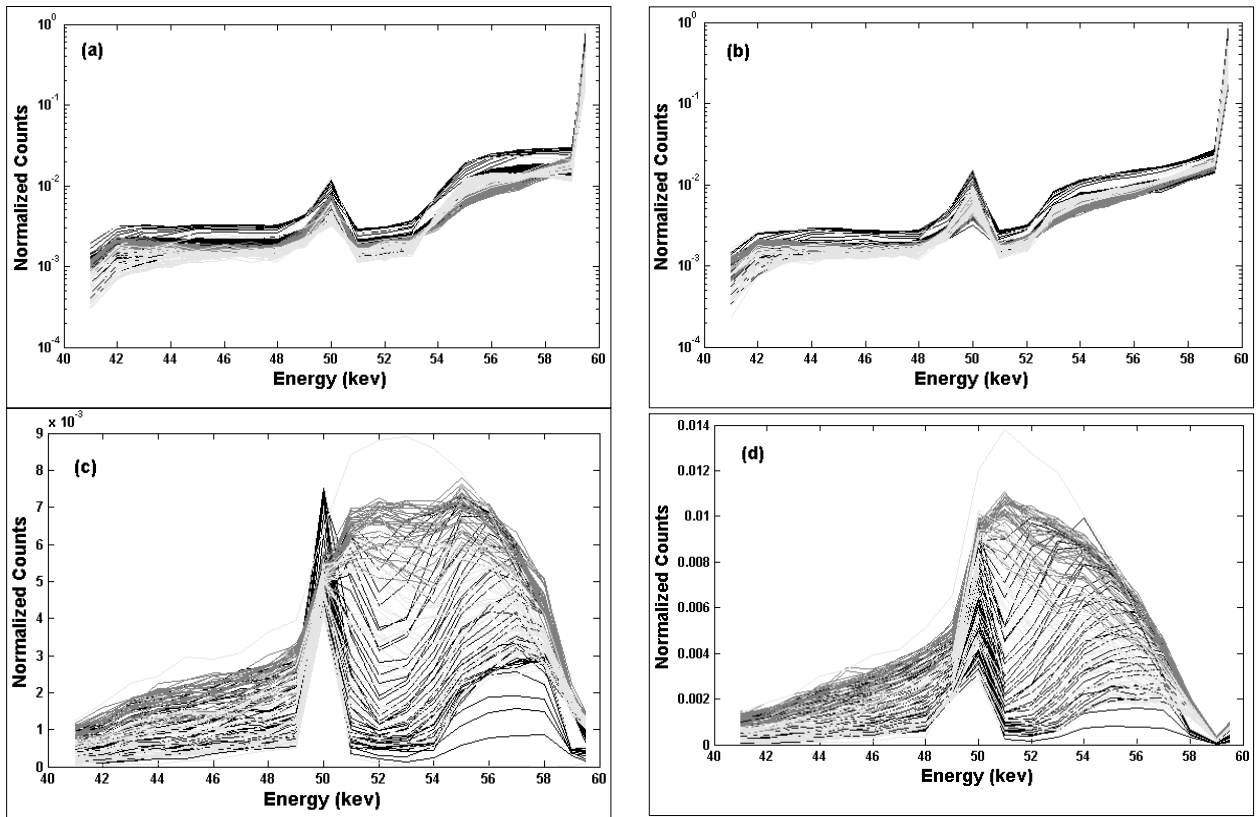


Fig. 2. Normalized spectra of various void fractions in various flow regimes at 40–60 keV energies. Reference of normalization was the highest spectrum (a). Black, grey and light grey graph are due to Annular, Bubbly and Droplet flow regimes. Detectors placed at 180° (a), 140° (b), 68° (c) and 52° (d) positions toward a source.

and the remaining were used for validation. The root mean square error (RMSE) is used for representing test data error. The RMSE of normalized test data for void fraction predicting is 0.0254. The predicted void fraction vs. the observed test data is shown in Fig. 3.

Another network that is used for classification of flow regime type has three output values 1, 2 and 3. These numbers specify Annular, Bubbly and Droplet flow regimes, respectively. But actual outputs of the network are not integer and should be rounded and then compared to the test data. The predicted flow regime

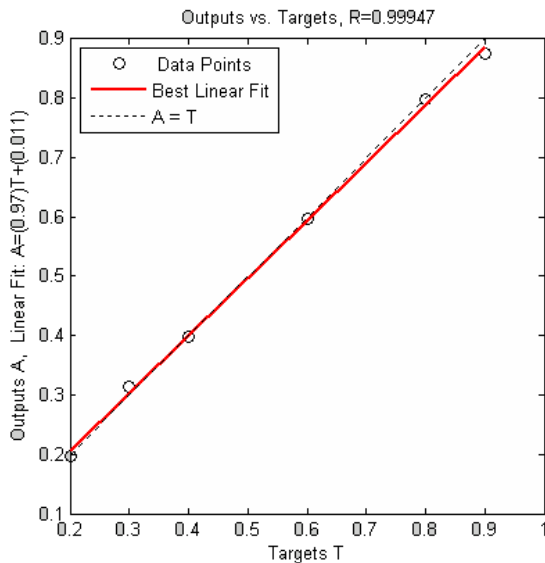


Fig. 3. Test data for void fraction.

vs. the observed test data is shown in Fig. 4. The result shows no error and all regime types of test data can be classified exactly.

Conclusions

The attenuation of 59.5 keV gamma-ray from ²⁴¹Am through the two-phase flow was measured by using CZT detector simulations. Several simulations are performed around the pipe on the same cross-section. Different

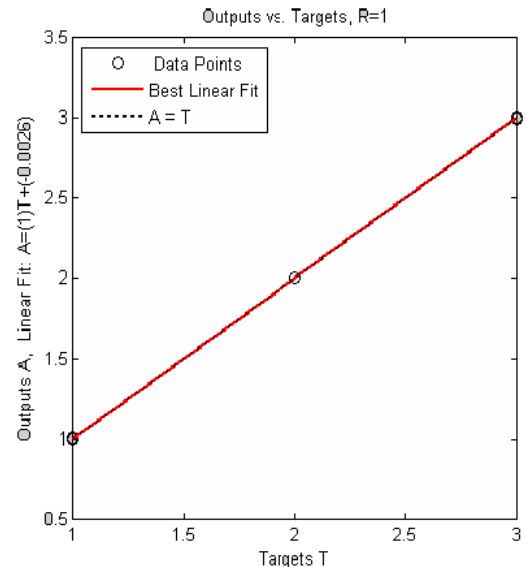


Fig. 4. Test data for flow regime.

spectra resultants from various flow regimes were calculated. Then, the simulated data were used as a training set for NNs. With responses from detectors, the average error in determination of the void fraction was 2.54%. All flow regimes were exactly identified. For vertical two-phase flows, it has been shown that neural networks are appropriate classifiers of flow regimes. This is especially useful when pipe lines are opaque. Thus, simulated data from the models appear to be suitable for training NNs. Results show that neural networks, in general, may be a promising tool for interpretation and analysis of two-phase flow data.

References

1. Abro E, Johanson GA (1999) Improved void fraction determination by means of multibeam gamma-ray attenuation measurements. *Flow Meas Instrum* 10:99–108
2. Beattie DRH (1972) Two-phase flow structure and mixing length theory. *Nucl Eng Des* 21:46–64
3. Briesmeister JF (1997) MCNP – A general Monte Carlo n-particle transport code. Version 4B. LA-126265, Los Alamos National Laboratory
4. Cember H, Johnson ET (2009) *Introduction to health physics*, 4th ed. McGraw-Hill Medical, New York
5. Haykin S (1999) *Neural network*, 2nd ed. MacMillan College Publishing Co, London
6. Hewitt GF (1978) *Measurement of two-phase flow parameters*. Academic Press, New York
7. Ishii M (1977) One-dimensional drift-flux model and constitutive equation for relative motion between phases in various two-phase flow regimes. *ANL* 77:37–47
8. Lahey RT, Banerjee S (1980) Advances in two-phase flow instrumentation. In: Lewins J, Becker M (eds) *Advances in nuclear science technology*. Vol. 13. Plenum Press, New York, pp 227–401
9. Levenberg K (1944) Method for the solution of certain nonlinear problems in least squares. *Q Appl Math* 2:164–168
10. Marquardt D (1963) An algorithm for least-squares estimation of nonlinear parameters. *SIAM Appl Math* 11:431–441
11. Priddy KL, Keller PE (2005) *Artificial neural networks: An introduction*. SPIE Press, Bellingham, WA, p 1
12. Sprowell RL, Phillips WA (1980) *Modern physics, the quantum physics of atoms, solids and nuclei*, 3rd ed. Wiley, New York